

A tunable multi-color "rainbow" filter for improved stress and dislocation field mapping in polycrystals using x-ray Laue microdiffraction

Odile Robach^{a*}, Jean-Sébastien Micha^b, Olivier Ulrich^a, Olivier Geaymond^c, Olivier Sicardy^d, Jürgend Härtwig^e, François Rieutord^a

^aCEA-Grenoble, INAC / SP2M / NRS, ^bUMR SPram CNRS-CEA-UJF, CEA-Grenoble, INAC, ^cCEA-LITEN, MINATEC Campus, ^{a,b,c}17 rue des Martyrs, 38054 Grenoble Cedex 9, France, ^dInstitut Néel, CNRS 25 rue des Martyrs, F-38042 Grenoble, France, ^eESRF, 6, rue Jules Horowitz, BP 220, 38043 Grenoble Cedex 9, France. E-mail: odile.robach@cea.fr

Synopsis

A technique to measure the energy profiles of Laue spots in x-ray Laue microdiffraction is presented. It uses a single-crystal diamond filter that attenuates several well-defined energies in the incident white-beam spectrum. A first application to lattice parameter measurements is demonstrated.

Abstract

White beam x-ray Laue microdiffraction allows fast mapping of crystal orientation and strain fields in polycrystals, with a submicron spatial resolution in two dimensions. In the well-crystallized parts of the grains, the analysis of Laue spots positions provides the local deviatoric strain tensor. In the parts with larger micro-misorientations, the spots shape and the orientation gradients (spots displacements) provide the density of unpaired dislocations (Geometrically Necessary Dislocations (GND's)). The hydrostatic part of the strain tensor, and the total dislocation density, may also be obtained, but more slowly, by measuring the energy profiles of the Laue spots using a variable-energy monochromatic beam. A new method is presented for the measurement of energy profiles, which offers mostly the same performances as the monochromatic method, with two advantages: i) the simultaneous measurement of the energy profiles and the Laue pattern; ii) the access to the energy profiles of a large number of spots with a small angular range. The method uses a thin rotating single crystalline diamond plate - the multi-color filter, installed upstream of the microfocussing optics. This diamond simultaneously diffracts a large number of discrete energies (forming a comb), and causes their attenuation in the - initially white - incident beam. The filter rotation causes a shift of the comb and allows to successively attenuate the various Laue spots of the sample. The position of the filtered-out energies at each rotation step is obtained from the diamond Laue pattern, measured with a second 2D detector. This article demonstrates the feasibility of the multi-color filter - "Rainbow" - method, and shows a first test of measurement of a known lattice parameter.

Keywords: x-ray; diffraction; microdiffraction; Laue; lattice expansion; energy profiles; white-beam; ESRF; strain

1. Introduction

Synchrotron radiation x-ray Laue microdiffraction using white beam has been used for more than a decade (Chung & Ice, 1999, MacDowell *et al.*, 2001, Kunz *et al.*, 2009, Ice & Barabash, 2007, Ice & Pang, 2009, Ulrich *et al.*, 2011, Maaß *et al.*, 2006, Ice *et al.*, 2004, Tamura *et al.*, 2000, 2002, 2003, Larson *et al.*, 2002, Kirchlechner *et al.*, 2010, 2011, Hofmann *et al.*, 2010) to determine the strain and orientation fields in polycrystalline materials, with a submicron spatial resolution, attempting to elucidate the relations between microstructure and mechanical properties. The existing instruments all offer the possibility to switch to monochromatic beam, to measure, via the photon energy, the position and width of the diffraction peaks along the radial direction of reciprocal space. The radial position provides an absolute measurement of the interplanar distance d_{HKL} of a given (HKL) spot. The radial width allows to access (with a few hypotheses) the total dislocation density, independently of the paired or unpaired character of the dislocations (Barabash & Ice, 2012). This is useful for incremental plastic deformation studies, to complement the white beam measurements of the transverse width, which is mostly sensitive to unpaired dislocations (GND's) (the total dislocation density is potentially detectable but only in the absence of GND's).

When the local crystalline quality is sufficient (misorientations < 1 mrad in the probe volume), the d_{HKL} measurement may be combined to the Laue pattern measurement to retrieve the 6 lattice parameters, and deduce the full elastic strain tensor. This combination requires to maintain the unit cell shape and orientation with respect to the incident beam perfectly constant between the two measurements. For the monochromatic method, this implies to re-position the beam on the sample with an accuracy better than the typical length on the sample corresponding to a variation of 10^{-4} on the orientation or the strain. The difficulty of this alignment led to develop a white beam method (Robach *et al.*, 2011) to simultaneously measure the Laue pattern on the 2D detector, and the energy of one spot using an energy-resolved point detector mounted on two translation stages. This method remains slow as the setting for the position of the point detector depends on the grain orientation: a prior analysis of the Laue pattern is necessary. This analysis is also necessary for the monochromatic method (unless long scans are used), for defining the incident energy.

This article describes the first tests of another method for measuring the energy position and width of the Laue spots, based on the concept of "multi-color filter": instead of using an incident beam with a single energy (as in the monochromatic mode), a white beam is used, in which several well-defined energies are missing. Hints that the method should work were already available: strong attenuations with high energy resolution (2 eV) were observed experimentally downstream of a diamond plate used for splitting the beam between the two branches of a beamline (Grübel *et al.*, 1994).

2. Experimental details

The experiments were performed using the Laue microdiffraction setup of the CRG-IF BM32 beamline at ESRF (Ulrich *et al.*, 2011). A schematic of the experimental setup is shown on Figure 1. The standard instrument features a micro-focusing optics, a xyz translation stage for the sample holder, inclined by 40 degrees with respect to the white incident beam (energy range 5-22 keV) and a 2D detector (#1) above the sample. Upstream of the focusing optics, a multi-color filter system was added, which includes the following elements: a vertical-gap slit to reduce the beam size

down to $0.3 \times 0.3 \text{ mm}^2$, followed by a motorized horizontal translation to bring the filter in and out of the beam. This stage carries a manual vertical translation stage, holding a motorized rotation stage (angle θ_f) with a horizontal axis nearly perpendicular to the incident beam (within 4-5 degrees), itself holding a single-crystalline thin diamond plate (the filter). The diamond plate of $3 \times 8 \text{ mm}^2$, with (110) orientation and $300 \text{ }\mu\text{m}$ thickness makes an angle of approximately 45 degrees with respect to the incident beam. This orientation allows to have two of the most intense diamond diffraction lines (the (111)'s) in the 9.5-12.5 keV range. A second 2D detector (#2) is placed upstream of the filter near $2\theta = 120$ degrees to collect the Laue patterns. This allows to calculate the energies of all the beams diffracted by the filter (including the ones not reaching the detector) for the various angular positions. This provides the energies that will be attenuated in the incident beam.

The filter was first mapped (installed in the sample position) by Laue microdiffraction, in order to check the absence of deviatoric strain of the unit cell ($< 2.10^{-4}$) and the homogeneity of the unit cell orientation (better than 0.2 mrad). It was then installed on the rotation stage, on the path of the incident beam. Scans in θ_f over 2.5 or 5 degrees with a 0.0025 degrees step were then performed, while recording on detector #1 the Laue patterns of the sample. Two samples were tested : a Germanium (111) single crystal wafer, and a polycrystalline bi-layer based of yttria-doped zirconia, forming the electrolyte and anode of a half - solid oxide fuel cell (SOFC). This sample was studied on the electrolyte side, which features grains of a few microns (Villanova et al. , 2010, 2011).

The orientation of the incident beam with respect to the crystal axes of the filter was chosen to be of low symmetry to be far away from degenerate conditions (when several diffracted beam have the same energy). This limits the occurrence of very closely-spaced dips, which are more difficult to analyze, in the intensity vs. θ_f curves of the sample's Laue spots. The effect of the filter insertion on the x-ray beam size was characterized and found negligible for the part of the spectrum above 9.7 keV. Figure 2 shows the profiles obtained by scanning a rectangular thin film of gold with well defined edges in front of the microbeam and measuring its fluorescence. The slope of the profile stays constant when inserting the filter.

3. Results

3.1. Germanium single crystal

Figure 3a shows the intensity vs. θ_f profiles for the 32 Laue spots of the Ge single crystal (over a total of 86 spots) that present one or several measurable extinctions over the scanned 5 degree range. The Laue patterns of the Ge sample and of the diamond filter are shown in Fig. 3b and 3c. The observed dips in Fig. 3a vary between 5 and 50%. The width of the dips varies between 0.0025 and 0.05 degrees in θ_f , illustrating the variations of energy resolution from one diamond line to the next. From Bragg's law, a variation of the Bragg angle $d\theta_{\text{Bragg}}$ produces a variation of energy of the diffracted ray of $dE = -E \cdot d\theta_{\text{Bragg}} / \tan(\theta_{\text{Bragg}})$. For an increment $d\theta_f$ of the filter angle, the ratio $d\theta_{\text{Bragg}} / d\theta_f$ can be calculated from the HKL of the line and the orientation of the incident beam with respect to the crystal. Several spots show an asymmetric shape or a "S"-shape, whose origin (probably linked to a dynamical effect) was not yet investigated.

Numerous extinctions are therefore available (here 68). Each dip potentially provides (via its minimum intensity position $\theta_{f,\text{dip}}(\text{HKL}_{\text{sample}})$, as a first approximation) one measurement of the

lattice expansion da/a of the Ge, when using an hypothesis of a cubic unit cell (i.e. assuming that the deviatoric strain is known). If this hypothesis is lifted, each (well chosen) combination of 6 θ_f measurements can potentially provide the 6 Ge lattice parameters.

For the purpose of measuring the da/a , the next stage in the analysis consists in comparing the experimental θ_f values of the dips to theoretical values. Figure 4 illustrates the method. In a plot of θ_f angle vs. diffracted beam energy, each dip corresponds to a crossing between two lines : a vertical line (with fixed energy) corresponding to the energy $E_{\text{theor_sample}}(\text{HKL}_{\text{sample}})$ of a given spot of the sample, and an inclined line (variable angle and energy) corresponding to the energy $E_{\text{theor_filter}}(\text{HKL}_{\text{filter}})$ of a given line of the filter during the θ_f rotation. Each spot from the sample may therefore undergo several extinctions, if the corresponding vertical line crosses several inclined lines. Each dip is therefore characterized by a couple $(\text{HKL}_{\text{sample}}, \text{HKL}_{\text{filter}})$.

Figure 4a was obtained from the orientations of the Ge and the diamond deduced from the Laue patterns (cf. Fig. 2b and 2c), the two unit cells being supposed cubic and of known lattice parameter (5.6575 \AA for Ge and 3.5668 \AA for diamond). More than 200 lines are expected between 5 and 22 keV for the filter, but only 64 lines are shown here, the ones with a theoretical intensity $(f_{\text{polarisation}} \cdot f_{\text{atomic}})^2$ larger than 0.1% of the intensity of the most intense line. The slope of the inclined lines directly provides the $dE/d\theta_f$ relative to each $\text{HKL}_{\text{filter}}$ line. The experimental positions of the dips are reported as dots on the figure, with the coordinates $(E_{\text{theor_sample}}(\text{HKL}_{\text{sample}}), \theta_{f,\text{dip}}(\text{HKL}_{\text{sample}}))$. The energies of the observed dips range from 9.5 to 18.9 keV. For the Ge (422) spot at 7 keV, the dip corresponds to the extinction of the (844) harmonic at 14 keV.

Figure 4a allows to establish a list of theoretical cross-points $(\text{HKL}_{\text{sample}}, \text{HKL}_{\text{filter}})$, and to attribute a $\text{HKL}_{\text{filter}}$ to each of the dips observed for a given HKL_{Ge} spot. Figure 4b details the method for converting the experimental dip angle $\theta_{f,\text{dip}}(\text{HKL}_{\text{sample}}, \text{HKL}_{\text{filter}})$ into a value of the experimental energy $E_{\text{exp}}(\text{HKL}_{\text{sample}})$: the experimental curve $E_{\text{theor}}(\text{HKL}_{\text{filter}}, \theta_f)$ is simply interpolated at $\theta_f = \theta_{f,\text{dip}}(\text{HKL}_{\text{sample}}, \text{HKL}_{\text{filter}})$. The normalized difference $dE/E = ((E_{\text{exp}}(\text{HKL}_{\text{sample}})/E_{\text{theor}}(\text{HKL}_{\text{sample}})) - 1)$ then provides the experimental $-da/a$ for this dip, measured with respect to a known "a" lattice parameter.

The direct application of this method to the 56 experimental dips for which the determination of $\text{HKL}_{\text{filter}}$ is totally clear leads to a mean dE/E of $-7.8.10^{-4}$, with a standard deviation of $\pm 16.3.10^{-4}$, and an amplitude of variation of $56.6.10^{-4}$, which is still far from the desired accuracy ($\pm 1.10^{-4}$). Already at this stage, the important noise level observed on the geometrical parameters of detector #2 led to fix these parameters to the mean value, and to refine only the diamond orientation. An uncertainty on the 5 geometrical parameters (3 for the 3D position of the probe volume, and 2 for the direction of the incident beam) was therefore expected. A refinement was therefore performed, using a criterion of minimization of the deviation of dE/E , on the two angles of the incident beam with respect to detector #2. This fit leads to a mean dE/E of $0.17.10^{-4}$, with a standard deviation of $2.51.10^{-4}$, and an amplitude of variation of $12.9.10^{-4}$, i.e. a significant improvement. The mean dE/E is therefore consistent with the lattice parameters given in the literature for Ge and diamond. Note that a da/a equally affecting the Ge and the diamond would go undetected by this method. The refined deviations (with respect to the fit on the Laue patterns) on the vertical and horizontal angles of the incident beam with respect to detector #2 are 0.7 and -1.2 mrad respectively. Figure 5 shows the $dE/E = (E_{\text{exp}}/E_{\text{theor}} - 1)$ of the various Ge Laue spots, vs. energy, after correcting the direction of the incident beam.

The analysis performed here is rather crude, and the obtained deviation on the dE/E should be perfectible by :

- smoothing the $E_{\text{theor}}(\text{HKL}_{\text{filter}}, \theta_f)$ curves (refinement of the initial orientation and the filter rotation axis) (4 parameters)
- using a more realistic hypothesis on the shape of the dips, in particular for those with an asymmetric or "S" shape
- improving the accuracy on the filter orientation : reducing the filter-detector #2 distance, and using a more realistic hypothesis on the shape of the diamond spots (to describe the elongation due to dynamical diffraction effect (Yan & Noyan, 2005)).
- using the integrated intensity of the Ge spots instead of the intensity of a single pixel.

As an element of comparison with the monochromatic method, the same diamond used as a monochromator set on the (-111) (see red line on Fig. 4a) would provide only 10 measurements of the da/a for an equivalent angular scan.

3.2. Solid Oxide Fuel Cell sample with micron-sized grains

The next test consisted in checking the applicability of the method to a sample with micron-sized grains. Figure 6 shows the intensity profiles vs. θ_f (cf. Fig. 3) for 32 of the 34 spots showing detectable attenuations for the SOFC sample. These spots are among the 173 most intense (out of around 500) of the multi-grain Laue pattern recorded on a single point of the sample. A photograph of the sample surface and the Laue pattern are also shown. Dip depths up to 60% are observed, indicating that the method should also work here. The analysis of the full local strain tensor for the grains in this sample will be described later. Here a single scan will cause extinctions on spots from several grains, i.e. the da/a of several grains will be measured, which is an advantage with respect to the method with the energy-resolved point detector, which studies the grains one by one. The simultaneous measurement of the Laue pattern is particularly useful here, as it provides a continuous check of the stability of the beam with respect to the sample during the energy measurements, which is crucial for a sample with very fine grains.

4. Conclusion and perspectives

This method provides fast energy measurements for numerous Laue spots, which should improve the accuracy on hydrostatic strain, thanks to the better statistics. The $\pm 2.5 \cdot 10^{-4}$ standard deviation obtained here between the different measurements of the germanium lattice parameter is certainly perfectible, the fine tuning of the experimental setup and data analysis remaining to be done.

For studying the full local elastic strain tensor, this method should allow :

- to improve the reliability of measurements performed by combining the Laue pattern (deviatoric strain) and the energy of one or several spots (absolute value of d_{HKL})
- to measure the full tensor using only spot energies (thanks to the large number of available energy measurements). This may allow to extend the domain of application of stress measurements to probe volumes with higher orientation gradients.
- to measure spot energies without prior analysis of the Laue pattern (the probability of finding dips in a 2.5 degree scan being about 7 times larger than with a monochromator)

The combination of continuous angular scans of the filter with a fast pixel detector (ex : Maxipix) installed near the 2D detector should allow fast mapping of both Laue pattern and energy profile.

For energy widths, the method will allow fast simultaneous measurements of dislocation densities for both paired and unpaired

dislocations. Short angular scans around a single dip should be sufficient, using the deepest and best-resolved dip (e.g. one associated to the $(-111)_{\text{filter}}$, which shows the largest $dE/d\theta_f$). One application should be the monitoring of the total dislocation density during in situ tensile and compressive mechanical tests of single-crystalline micro-pillars (Kirchlechner et al., 2010, 2011, Maaß et al. 2006), which require fast measurements without sample motion. This should facilitate the monitoring of the first glide system, which is often difficult to detect through spot elongation in the Laue patterns, as it gives few GND's compared to secondary systems.

An alternative name of "Batterman filter" was proposed for the method.

Acknowledgements

We thank the CEA-CNRS staff of the BM32 beamline for technical help with the microdiffraction setup, the ESRF for providing the x-ray beam, P. Gergaud, O. Castelnaud, G. Renaud, and T. Zhou for participation in the preliminary discussions, H. Isern et P. Montmayeul for technical support, and N. Tamura for suggesting the alternative name for the method. Financial support was provided by the AMOS ANR project led by J.L Rouvière. Laue pattern analysis was performed using the LaueTools software (LaueTools web site).

References

- Barabash, R.I., Ice, G.E. (2012) "Chapter 1 : diffraction analysis of defects : state of the art" in "Strain and dislocation gradients from diffraction", Barabash R.I., Ice G.E., Eds, Imperial College Press / World Scientific Publishing (to be published)
- Chung, J.-S., Ice, G.E. (1999). *J. Appl. Phys.* **86** 5249-5255
- Grübel, G., Als-Nielsen, J., Freund, A.K. (1994). *Journal de Physique IV, Suppl.*, **4**, C9-27
- Hofmann, F., Abbey, B., Song, X., Dolbnya, I., Korsunsky, A.M. (2009). *Int. J. Mod. Phys. B*, **24**, 279-287
- Ice, G.E., Barabash, R.I. (2007) Chapter 79 : White Beam Microdiffraction and Dislocations Gradients" in *Dislocations in Solids*, F.R.N. Nabarro, J.P. Hirth, eds., Elsevier, 499 - 601
- Ice G.E, Larson, B.C., Yang, W., Budai, J.D., Tischler, J. Z., Pang, J.W.L., Barabash, R.I., Liu, W. (2004). *J. Synchrotron Rad.* **15**, 155-162
- Ice, G.E, Pang, J.W.L. (2009) *Mat. Charact.* **60**, 1191-1201
- Kirchlechner, C., Kiener, D., Motz, C., Labat, S., Vaxelaire, N., Perroud, O., Micha, J.S., Ulrich, O., Thomas, O., Dehm, G., Keckes, J. (2010) *Phil. Mag.* **91**, 1256-1264
- Kirchlechner C., Keckes J., Micha J.S., Dehm G. (2011) *Advanced Engineering Materials* **13**, 837.
- Kunz, M., Tamura, N., Chen, K., MacDowell, A.A., Celestre, R.S., Church, M.M., Fakra, S., Domning, E.E., Glossinger, J.M., Kirschman, J.L., Morrison, G.Y., Plate, D.W., Smith, B.V., Warwick, T., Yashchuk, V.V., Padmore, H.A. (2009) *Rev. Sci. Instr.* **80**, 035108
- Larson, B. C., Yang, W., Ice, G. E., Budai, J. D., Tischler, J. Z. (2002). *Nature (London)* **415**, 887-890.
- LaueTools. <http://sourceforge.net/projects/lauetools/>
- Maaß, R., Grolimund, D., Petegem, S. V., Willimann, M., Jensen, M., Swygenhoven, H. V., Lehnert, T., Gijs, M. A. M., Volkert, C. A., Lilleodden, E. T., Schwaiger, R. (2006). *Appl. Phys. Lett.* **89**, 151905
- MacDowell, A.A., Celestre, R.S., Tamura, N., Spolenak, R., Valek, B.C., Brown, W.L., Bravman, J.C., Padmore, H.A., Batterman B.W., Patel, J.R. (2001). *Nucl. Instrum and Methods Phys. Res. A* **467-468**, 936-943
- Yan, H., Noyan, I.C. (2005) *J. Appl. Phys.* **98**, 073527
- Robach, O., Micha, J.-S., Ulrich, O., Gergaud, P. (2011) *J. Appl. Cryst.* **44**, 688-696
- Tamura, N., MacDowell, A. A., Spolenak, R., Valek, B. C., Bravman, J. C., Brown, W. L., Celestre, R. S., Padmore, H. A., Batterman, B. W., Patel, J. R. (2003). *J. Synchrotron Rad.* **10**, 137-143

Tamura, N., MacDowell, A. A., Celestre, R. S., Padmore, H. A., Valek, B. C., Bravman, J. C., Spolenak, R., Brown, W. L., Marieb, T., Fujimoto, H., Batterman, B. W., Patel, J. R. (2002). *Appl. Phys. Lett.* **80**, 3724
 Tamura, N., Valek, B. C., Spolenak, R., MacDowell, A. A., Celestre, R. S., Padmore, H. A., Brown, W. L., Marieb, T., Bravman, J. C., Batterman, B. W., Patel, J. R. (2000). *Mat. Res. Soc. Symp. Proc.* **612**, D.8.8.3-D8.8.6
 Ulrich, O., Biquard, X., Bleuet, P., Geaymond, O., Gergaud, P., Micha, J.S., Robach, O., Rieutord, F. (2011) *Rev. Sci. Instr.* **82**, 033908
 Villanova, J., Sicardy, O., Fortunier, R., Micha, J.S., Bleuet, P. (2010). *Nucl. Instrum. Methods Phys. Res. B*, **268**, 282-286
 Villanova, J., Sicardy, O., Fortunier, R., Micha, J.-S., Bleuet, P. (2011) *Materials Science Forum* 681, 25-30

5. Figure Captions

Figure 1 Experimental setup : the multi-color filter setup (vertical gap slit, x translation, z translation, θ_f rotation, 2D detector #2 at $2\theta = 120$ degrees in a vertical diffraction plane) is placed about 1 m upstream of the Laue microdiffraction setup (H and V gap slits, Kirkpatrick-Baez mirrors for micro-focusing, xyz sample translation stage, sample at 40 degrees, 2D detector #1 at $2\theta = 90$ degrees in a vertical diffraction plane). The filter creates numerous well-defined dips in the energy spectrum of the incident beam. These dips shift in energy with the rotation, and successively attenuate the various Laue spots of the sample.

Figure 2 Effect of the insertion of the filter on the size of the x-ray micro-beam. Fluorescence profiles on a thin rectangular gold layer on silicon, without (black symbols) and with (red symbols) the filter. The x translation is horizontal and perpendicular to the incident beam. The y translation is at 40 degrees of the incident beam, in the vertical plane containing the beam. Beam size (x,y) : (0.8, 1.7) μm .

Figure 3 Measurements on the Ge single crystal : (a) monitoring of 32 of the 86 Laue spots of Ge, during a variation of 5 degrees of the θ_f angle of the filter. For each spot, the intensity of a fixed pixel is plotted (the pixel of maximum intensity at $d\theta_f = 0$). Intensities are normalized to their values at $d\theta_f = -2.5$ degrees. The curves are shifted vertically by 50%. (b,c) : Laue patterns of the Ge sample (b) (micro-beam, detector #1) and the diamond filter (macro-beam, detector #2, $d\theta_f = 0$ (blue) and $d\theta_f = 0.5$ degrees (red)).

Figure 4 (a) : calculated energies of the Ge and diamond diffracted beams from the experimental Laue patterns, in an energy vs. filter angle plot. For the diamond the energies changes at each angle point in the scan. The cross points between the energies of the diamond diffracted beams (inclined lines) and the energies of the Ge spots (vertical lines) give the theoretical θ_f value of each dip of each Ge spot. The color code shows the theoretical intensity of the diamond diffracted beams (an estimate of the dip depth), in fractions of the intensity of the most intense beam. The circles mark the 68 dips experimentally detected on 32 of the Ge spots. (b) interpolation used to convert the experimental angle position of a dip into an experimental energy $E_{\text{exp}}(\text{HKL}_{\text{sample}})$, after having attributed the dip to a given $\text{HKL}_{\text{filter}}$ ray using (a).

Figure 5 The 56 measurements of the Ge lattice parameter, expressed in $dE/E = -da/a$ with respect to the theoretical lattice parameter of 5.6575 Å, as deduced from the positions of the dips in Fig. 3, vs. the Ge spot energy. The color code is the same as the one of Fig. 2a (estimated dip depth). Each type of symbol corresponds to a given $\text{HKL}_{\text{filter}}$. Each vertical line corresponds to a given $\text{HKL}_{\text{sample}}$.

Figure 6 Measurements on a polycrystal with micron-sized grains (electrolyte side of a "half" solid-oxide-fuel-cell). The x-ray microbeam is at a fixed position with respect to the sample. (a) monitoring of the intensity of 32 Laue spots from several SOFC grains, during a variation of 2.5 degrees of the filter angle (see Figure 3 for details). The curves are vertically shifted by 60%. (b) optical microscope image $30 \times 20 \mu\text{m}^2$. (c) positions of the 173 most intense Laue spots of the multi-grains Laue pattern.

Fig 1 :

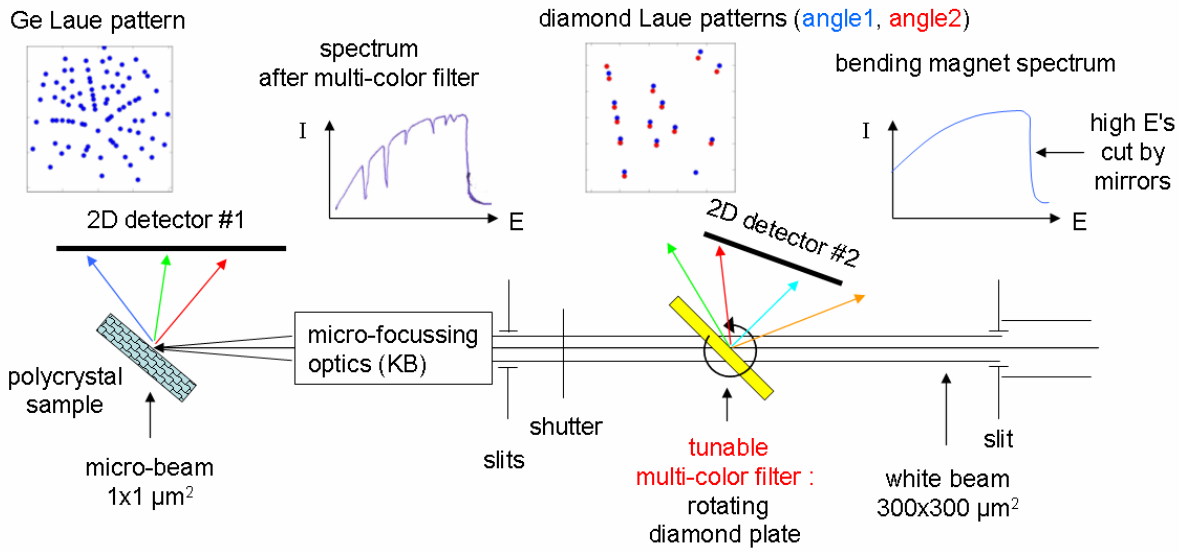


Fig 2 :

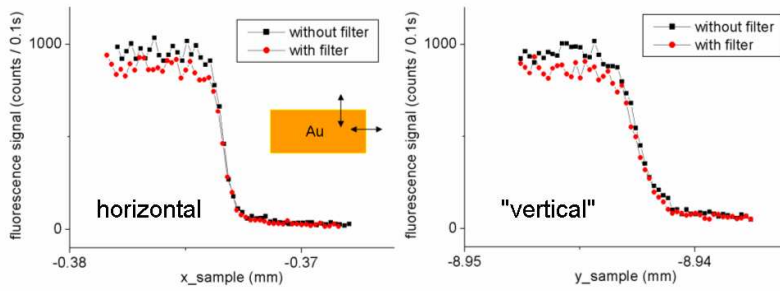


Fig. 3a :

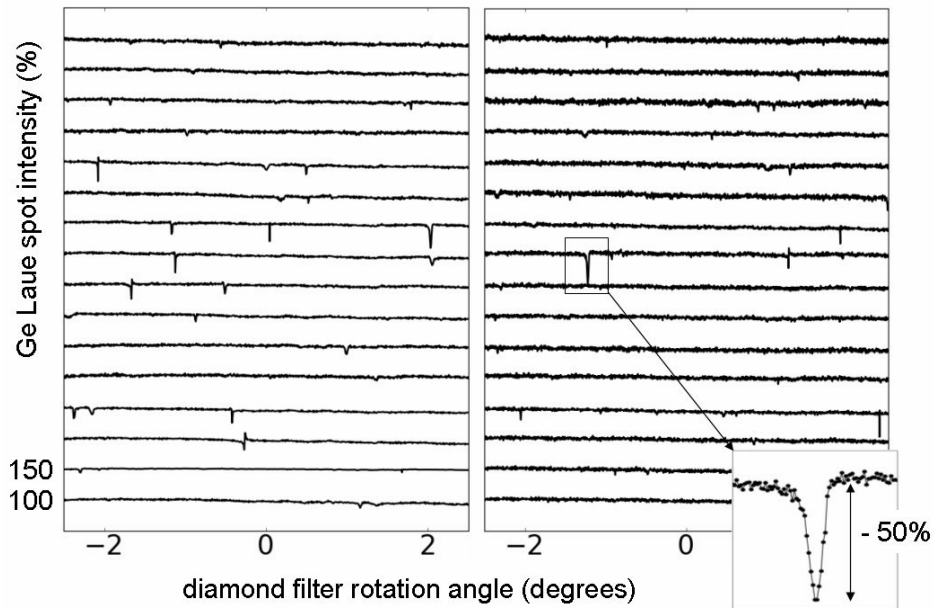


Fig. 3b, c :

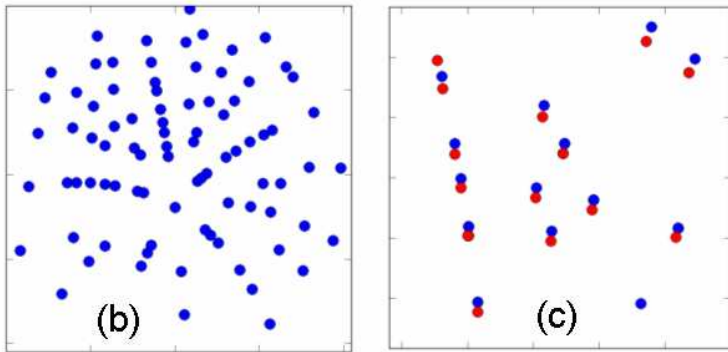


Fig. 4a :

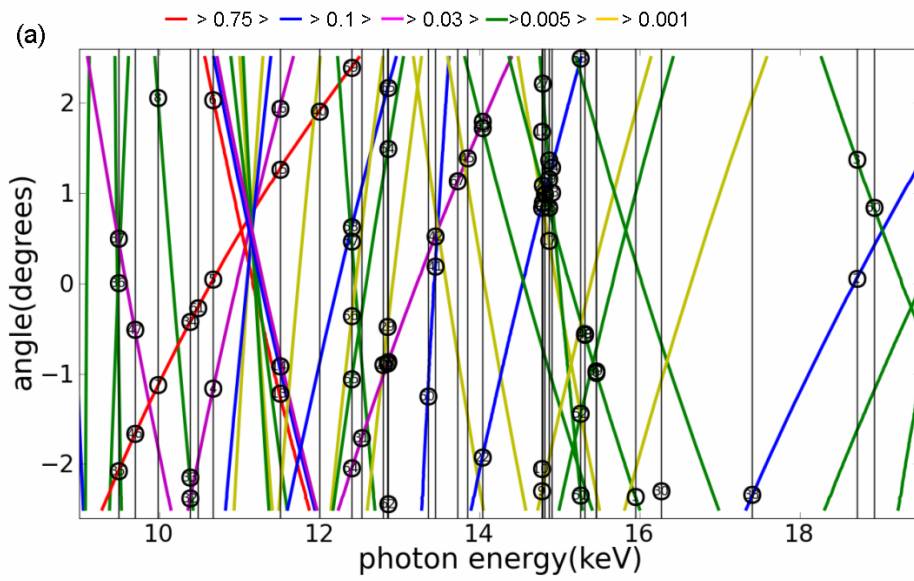


Fig. 4b :

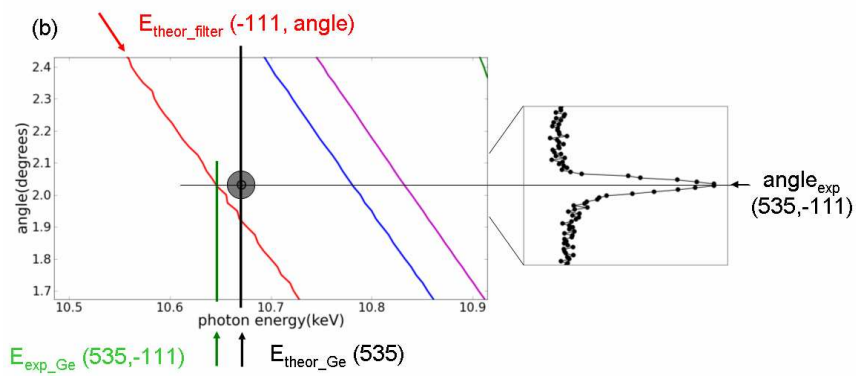


Fig. 5 :

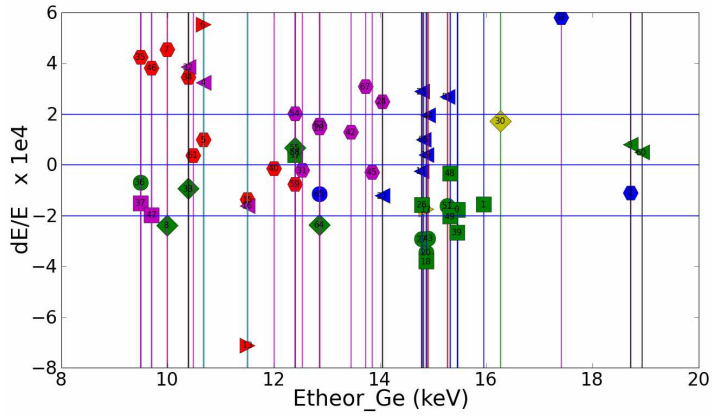


Fig. 6a :

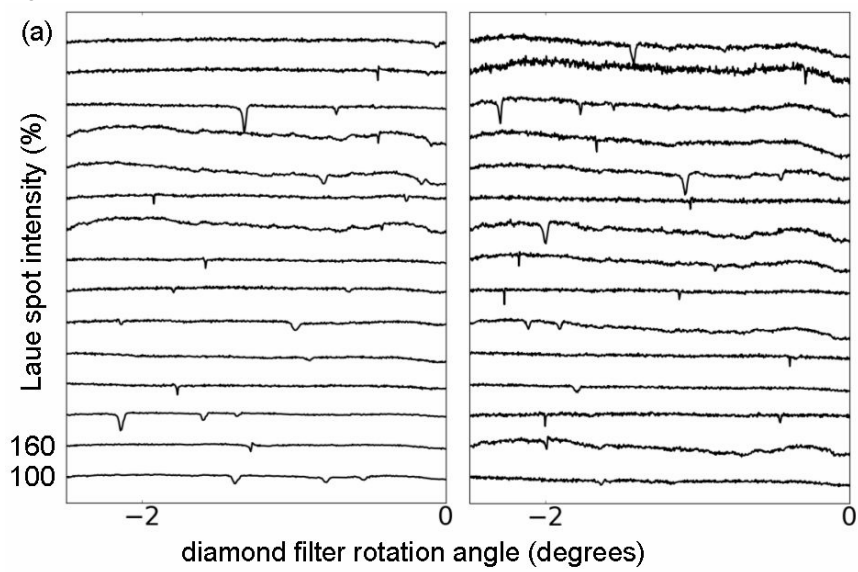


Fig. 6b,c :

